

This work was written as part of one of the author's official duties as an Employee of the United States Government and is therefore a work of the United States Government. In accordance with 17 U.S.C. 105, no copyright protection is available for such works under U.S. Law.

Public Domain Mark 1.0

<https://creativecommons.org/publicdomain/mark/1.0/>

Access to this work was provided by the University of Maryland, Baltimore County (UMBC) ScholarWorks@UMBC digital repository on the Maryland Shared Open Access (MD-SOAR) platform.

Please provide feedback

Please support the ScholarWorks@UMBC repository by emailing scholarworks-group@umbc.edu and telling us what having access to this work means to you and why it's important to you. Thank you.

RESEARCH ARTICLE | APRIL 21 2011

Range, resolution and power of THz systems for remote detection of concealed radioactive materials

G. S. Nusinovich; P. Sprangle; C. A. Romero-Talamas; V. L. Granatstein



J. Appl. Phys. 109, 083303 (2011)

<https://doi.org/10.1063/1.3572062>

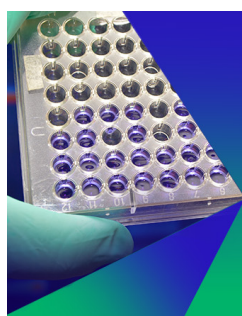


View
Online



Export
Citation

CrossMark



Biomicrofluidics

Special Topic:
Microfluidics and Nanofluidics in **India**

Submit Today

Range, resolution and power of THz systems for remote detection of concealed radioactive materials

G. S. Nusinovich,^{1,a)} P. Sprangle,² C. A. Romero-Talamas,¹ and V. L. Granatstein¹

¹*Institute for Research in Electronics and Applied Physics, University of Maryland, College Park, Maryland 20742-3511, USA*

²*Plasma Physics Division, Naval Research Laboratory, Washington, DC 20375-5320, USA*

(Received 12 January 2011; accepted 3 March 2011; published online 21 April 2011)

This paper analyzes parameters required for realizing remote detection of a concealed source of ionizing radiation by observing the occurrence of breakdown in air by a focused wave beam. Production of free electrons and the free electron density in the absence/presence of additional sources of ionization are analyzed. The maximum electron density in the discharge and the time required for this density to return after the discharge back to its stationary level, are estimated. The optimal excess of the power density and the corresponding power level as the function of frequency are determined. It is shown that the optimal frequency of such systems ranges from 0.3 up to 0.8 THz. The paper also determines the range of such systems as the function of the source frequency and power and contains a brief analysis of available sources of microwave, millimeter-wave and THz radiation. © 2011 American Institute of Physics. [doi:10.1063/1.3572062]

I. INTRODUCTION

Just recently, a new method was proposed^{1–3} for the remote detection of concealed radioactive materials. This method is based on focusing a high-power electromagnetic (EM) wave beam in a small volume of air where the wave electric field exceeds the breakdown threshold and, therefore, in the presence of free electrons an avalanche discharge can be initiated. When the wavelength is short enough, the probability of having even one free electron in this volume is very small. Hence, initiation of the discharge indicates that in the vicinity of this volume there are some materials causing ionization of air. Below, we analyze, first, the rate equations describing populations of free electrons and negative ions and, then, study the dependence of range and resolution of such systems on the frequency and power of the EM radiation.

II. ELECTRON AND ION DENSITIES. PRODUCTION OF FREE ELECTRONS

In the prebreakdown stage, i.e., in the absence of EM radiation, the electron density N_e and the negative ion density N_- can be found from rate equations:⁴

$$\frac{\partial N_e}{\partial t} = \alpha_{RM}Q + \beta_{det}NN_- - v_{att}N_e - v_{rec,i-e}N_+N_e, \quad (1)$$

$$\frac{\partial N_-}{\partial t} = v_{att}N_e - \beta_{det}NN_- - v_{rec,i-i}N_+N_-. \quad (2)$$

In Eqs. (1) and (2), Q is the ambient ionization rate at a near ground level (below, we assume Q to be close to 20 pairs/cm³-s), $\alpha_{RM} > 1$ is the ionization enhancement factor due to radioactive materials (in their absence $\alpha_{RM} = 1$), β_{det} is the detachment rate by nitrogen and oxygen molecules in air (typically the contribution from oxygen dominates) and N is

the density of air molecules (at the room temperature and atmospheric pressure $\beta_{det}N \approx 30$ s⁻¹), v_{att} is the electron attachment rate (at room temperature $v_{att} \approx 8 \times 10^7$ s⁻¹), $v_{rec,i-e}$ and $v_{rec,i-i}$ are the ion-electron and ion-ion recombination rates, respectively ($v_{rec,i-e} \approx 3 \times 10^{-8}$ cm³/s, $v_{rec,i-i} \approx 2 \times 10^{-6}$ cm³/s). Also in Eq. (1), N_+ is the density of positive ions; in a quasineutral discharge $N_+ = N_- + N_e$.

In a stationary state, Eqs. (1) and (2) yield $\alpha_{RM}Q = v_{rec,i-e}N_+N_e + v_{rec,i-i}N_+N_-$. Since the rate of ion-ion recombination greatly exceeds the rate of ion-electron recombination and also the negative ion density is much larger than the free electron density, the first term in the rhs of this equation can be omitted. Then, assuming $N_+ \approx N_-$, the density of negative ions can be estimated as $N_- \approx \sqrt{\alpha_{RM}Q/v_{rec,i-i}}$. When $\alpha_{RM} = 1$, $Q = 20$, and $v_{rec,i-i} \approx 2 \times 10^{-6}$ cm³/s, this yields the density of negative ions $\approx 3 \times 10^3$ cm⁻³. Correspondingly, the density of free electrons can be defined as

$$N_e(\text{cm}^{-3}) \approx 10^{-3} \left\{ \frac{3}{8} \sqrt{10\alpha_{RM}} + \frac{1}{4} \alpha_{RM} \times 10^{-3} \right\}. \quad (3)$$

Here the second term in figure brackets can be ignored; hence this density is proportional to $\sqrt{\alpha_{RM}}$. So, when α_{RM} varies from 1 (no radioactive materials) to 10², this density varies from 10⁻³ cm⁻³ to 10⁻² cm⁻³. This density is rather low; however, the production rate of free electrons can be rather large. This rate is primarily determined by the second term in the right-hand side of Eq. (1). For parameters given above this yields

$$\Delta N_e(\text{cm}^{-3}) = 9 \times 10^4 \sqrt{\alpha} \Delta t(s). \quad (4)$$

Hence, for example, in the absence of additional ionization, during a 10 μ s pulse there will be about one free electron born in one cubic centimeter. Note that the lifetime of these electrons determined by the attachment rate [third term in Eq. (1)] is more than 10 ns which is long enough for initiating the avalanche process.

^{a)}Author to whom correspondence should be addressed. Electronic mail: gregoryn@umd.edu.

III. TYPICAL TIMES OF TRANSITION PROCESSES

The time required for electron density to exponentially grow in the discharge from the initial very low level to saturation where the plasma frequency is close to the wave frequency depends on the effective ionization rate $\nu_{i,\text{ion}}$. The corresponding dependence of the pulse duration required for reaching the saturation in the case of electron density in the prebreakdown stage on the order of 10^{-3} cm^{-3} can be given⁵ as

$$\tau_\mu \approx \frac{4.6}{\nu_{i,\text{eff}}(\hat{P})} \{9.04 + \log[f(\text{THz})]\}. \quad (5)$$

The effective ionization rate $\nu_{i,\text{ion}}$, which is the difference between the ionization rate and the rate of electron attachment to the molecular oxygen, depends on the excess of the wave power density over its threshold. This dependence was calculated with the use of a Fokker–Planck kinetic code in Refs. 5 and 2; for $\hat{P} \leq 2$ the effective ionization frequency is less than 10^9 s^{-1} . So, the pulse duration required for breakdown saturation at THz frequencies is less than 20 ns. Note that the power density is nonuniform in the volume where the radiation is focused and is maximum just at the center in the focal plane. This is the region where the time required to reach saturation is the shortest. For diagnostic purposes, the pulse duration should slightly exceed this value; then the THz signal can be reflected from the volume where the discharge is saturated and, hence, can be detected by a receiver. Since in the saturated discharge $N_e(\text{cm}^{-3}) \approx 10^{15} [f(\text{THz})]^2$,⁵ for near terahertz frequencies the maximum electron density is on the order of 10^{15} cm^{-3} .

Equation (1) also allows one to estimate the time required for electron density to drop from its maximum value back to its stationary value after breakdown. As follows from Eq. (1), $N_e(t) \approx N_{e,\text{max}} \exp(-\nu_{\text{att}} t)$. Thus, for $\nu_{\text{att}} \approx 8 \times 10^7 \text{ s}^{-1}$ it takes $< 1 \text{ } \mu\text{s}$ for the electron density to go from 10^{15} cm^{-3} down to 10^{-3} cm^{-3} .

So far, we have neglected aerosols, which are important for maritime environment. The presence of atmospheric aerosols can significantly reduce the ion density. Aerosols range in size from less than $0.01 \text{ } \mu\text{m}$ to over a $1 \text{ } \mu\text{m}$, and their density can range from $\sim 10^2 \text{ cm}^{-3}$ to $\sim 10^5 \text{ cm}^{-3}$. If ions collide with aerosols, their charge may be transferred to the aerosols. So the ion density rate equation should describe the loss of ions due to charge attachment to the aerosols. Since many types of aerosols are hygroscopic, their radius and the aerosol attachment coefficient increase with the humidity.

IV. REQUIRED POWER

Let us now evaluate the required power of the EM radiation source. Assume that this radiation propagates as a wave beam³ having in the focal plane the radial profile

$$|E(r)|^2 = E_0^2 \exp\left\{-2\frac{r^2}{\rho_0^2}\right\}. \quad (6)$$

Here the wave beam width in a focal plane depends on the distance L from an antenna of the radius R :

$$\rho_0 = \frac{1}{\sqrt{\pi}} \frac{L}{R} \lambda. \quad (7)$$

Such a wave beam first converges due to the focusing by antenna and then diverges due to diffraction. The power density exceeds the breakdown threshold in the volume³

$$V = \frac{\pi^2 \rho_0^4}{3 \lambda} \left\{ \frac{2}{3} (5 + \hat{P}) \sqrt{\hat{P} - 1} - 4 \arctan(\sqrt{\hat{P} - 1}) \right\}. \quad (8)$$

In Eq. (8), $\hat{P} = P/P_{\text{th}}$ is the ratio of the wave power to its threshold value in a focal plane. When $\hat{P} - 1 = \tilde{p} \ll 1$, the function in figure brackets of (8) can be approximated as $2\tilde{p}^{3/2}$.

The power in a wave beam and the wave amplitude on axis E_0 are related as

$$P = p_{\text{max}} (\pi \rho_0^2 / 2). \quad (9)$$

In Eq. (9) $p_{\text{max}} = E_0^2 / 2Z_0$ is the power density on axis ($Z_0 = 377 \text{ } \Omega$ is the wave impedance of free space). The breakdown is possible in the region where the wave intensity exceed the breakdown threshold,

$$E_0^2 \exp\{-2(r^2/\rho_0^2)\} \geq E_{\text{th}}^2. \quad (10)$$

Equations (9) and (10) define the relation between the width of the wave beam ρ_0 and the radius of the area where the field exceeds the threshold in the focal plane (cf. Ref. 3):

$$r_{\text{th}} = \rho_0 \sqrt{\ln(2P/\pi \rho_0^2 p_{\text{th}})/2}. \quad (11)$$

The threshold value E_{th} at the atmospheric pressure is equal to^{5,6}

$$E_{\text{th}}(\text{MV/m}) = 3.2 \sqrt{1 + \omega^2/\nu_{\text{coll}}^2}. \quad (12)$$

In Eq. (12), ω is the wave frequency and $\nu_{\text{coll}} = 4.3 \times 10^{12} \text{ Hz}$ is the effective collision frequency. Correspondingly, the threshold power density $p_{\text{th}} = E_{\text{th}}^2 / 2Z_0$ is equal to

$$p_{\text{th}}(\text{MW/cm}^2) = 1.36 \left\{ 1 + 2.135 [f(\text{THz})]^2 \right\}. \quad (13)$$

Since the total power required for initiating the breakdown is $P_{\text{th}} = p_{\text{th}} (\pi \rho_0^2 / 2)$, we can rewrite Eq. (11) as $r_{\text{th}} = \rho_0 \sqrt{\ln(\hat{P})/2}$ and then come back to Eq. (8) and rewrite it as

$$\begin{aligned} V &= \frac{4}{3\lambda} \left[\frac{P}{p_{\text{th}}} \right]^2 \frac{1}{\hat{P}^2} \left\{ \frac{2}{3} (5 + \hat{P}) \sqrt{\hat{P} - 1} - 4 \arctan(\sqrt{\hat{P} - 1}) \right\} \\ &= \frac{4}{3\lambda} \left[\frac{P}{p_{\text{th}}} \right]^2 \Phi(\hat{P}). \end{aligned} \quad (14)$$

The function $\Phi(\hat{P})$, which is the volume normalized to $(4/3\lambda)(P/p_{\text{th}})^2$, is shown in Fig. 1. Its maximum (about 0.415) corresponds to the power-to-threshold ratio $\hat{P}_{\text{opt}} \approx 2.75$. This value defines the optimal width of the wave beam:

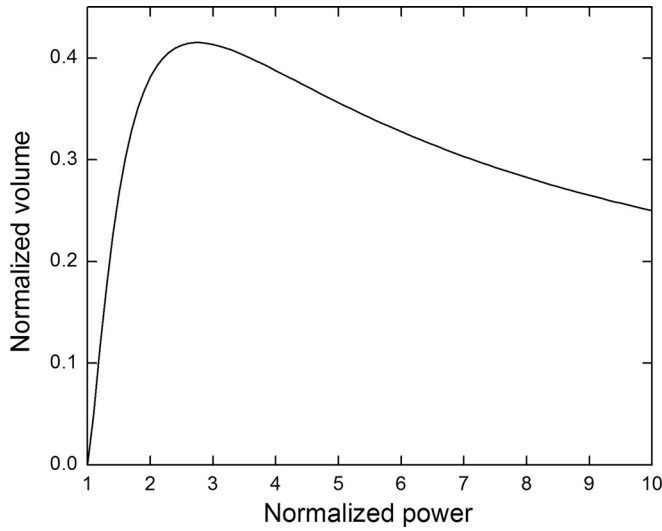


FIG. 1. The dependence of the function which determines the volume occupied by the focused EM radiation on the wave beam power normalized to its breakdown threshold value.

$$\rho_{0,\text{opt}} \approx 0.48 \sqrt{P/p_{\text{th}}}. \quad (15)$$

The power required to create the wave excess over breakdown threshold in such a volume, as follows from Eqs. (13) and (14), can be given as

$$P_{\text{opt}}(\text{MW}) \approx .317 \sqrt{V(\text{cm}^3)} \frac{1 + 2.135[f(\text{THz})]^2}{\sqrt{f(\text{THz})}}. \quad (16)$$

With the frequency increase this power decreases in the range $\omega^2 \ll v_{\text{coll}}^2$, but then it increases when $\omega^2 \gg v_{\text{coll}}^2$. The optimal frequency defining the bottom of the Paschen curve for air at the atmospheric pressure is close to 0.4 THz. A corresponding dependence of the required power on the frequency is shown in Fig. 2 for several values of the volume where the radiation should be localized.

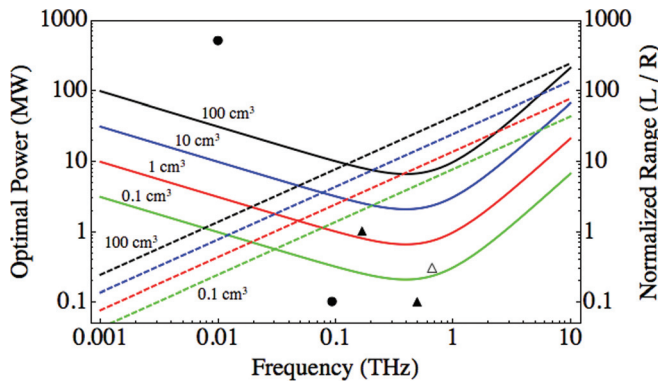


FIG. 2. (Color online) The source power (solid lines) and the range-to-antenna radius ratio (dashed lines) as functions of the wave frequency for several values of the volume in which breakdown conditions are fulfilled. The solid circle at 0.01 THz frequency shows parameters of the backward-wave oscillator used in NAGIRA; the solid circle at about 0.1 THz frequency shows parameters of the W-band gyro-amplifier used in the millimeter-wave radar WARLOC; the solid triangle at 0.17 THz frequency shows the 1 MW cw gyrotron for the international tokamak ITER; the solid triangle at 0.5 THz frequency shows the 100 kW gyrotron with a pulsed solenoid; finally an empty triangle shows the 0.67 THz, 300 kW gyrotron under development at the University of Maryland.

V. RANGE AS THE FUNCTION OF FREQUENCY AND POWER

Let us now analyze the possible range of such systems. The range or, more exactly, the ratio of the focal distance to the radius of the radiating antenna is given by Eq. (7) where the optimal waist of the wave beam is given by Eq. (15). This ratio scales as

$$L/R \propto \rho_0 \propto \sqrt{P}. \quad (17)$$

In the case of the optimal power given by Eq. (16) this ratio is equal to

$$\left(\frac{L}{R}\right)_{\text{opt}} \approx 43.3 \left[\frac{V(\text{cm}^3)}{100}\right]^{1/4} [f(\text{THz})]^{3/4}. \quad (18)$$

Equation (18) shows that, when the maximum size of the antenna dish is fixed, the system range increases with the operating frequency. The dependence of this range-to-antenna radius ratio on the frequency for several values of the volume is also shown in Fig. 2. As follows from Fig. 2, at frequencies below 10 GHz only short-focused operation is possible—the range should be on the order of the antenna size or less. To have a reasonably large range, a system should operate at sub-THz frequencies and above.

VI. AVAILABLE SOURCES OF HIGH-POWER RADIATION

Available sources of microwave, millimeter-wave and terahertz radiation are discussed elsewhere (Ref. 7). In Fig. 2 only two data points described in Ref. 7 are shown by solid circles: a repetitively pulsed X-band (10 GHz), 500 MW backward-wave oscillator used in the nanosecond gigawatt radar (NAGIRA),⁸ and a W-band (95 GHz) gyro-amplifier delivering 100 kW peak and 10 kW average power in the WARLOC radar.⁹ The solid triangle at 0.17 THz represents a 1 MW continuous-wave gyrotron;¹⁰ the solid triangle at 0.5 THz represents a 100 kW gyrotron with pulsed solenoid.¹¹ An empty triangle shows a 670 GHz gyrotron with a pulsed solenoid designed to deliver 300 kW³ which can create the field exceeding the threshold in about 0.16 cm³ volumes.

Practically all sources shown in Fig. 2 have pulse duration longer than 100 ns, except for the one for NAGIRA where the pulse duration was intentionally made short (5 ns). So, one can use a series of 40–50 ns pulses and expect that their last part, after creation of the discharge with high enough plasma density, will be reflected back and, hence, registered.

VII. SUMMARY

Above, we gave an estimate for the production rate of free electrons. As shown in Ref. 3, a 670 GHz, 300 kW gyrotron which is currently under development allows one to realize in the presence of free electrons the breakdown in the volume of 0.16 cm³. This gyrotron is designed to operate in 10 μs pulses. As follows from Eq. (4), in the absence of radioactive materials, the probability to have one seed electron

in this volume during one such pulse is about 14%, i.e. one breakdown event will be observed in seven shots. When radioactive materials increase the production rate α_{RM} by a factor of 10, this probability becomes close to 45%, i.e. one event will be observed in two shots.

ACKNOWLEDGMENTS

This work has been supported by the Office of Naval Research under Grant No. 000140911190. Stimulating discussions were held with T. M. Antonsen, Jr., G. M. Milikh, and J. Rynes.

¹G. S. Nusinovich, V. L. Granatstein, T. M. Antonsen, Jr., R. Pu, O. V. Sinit-syn, J. Rodgers, A. B. Mohamed, J. Silverman, M. Al-Sheikhly, and Y. S. Dimant, IEEE, Int. Vacuum Electronics Conf., (IEEE, Piscataway, NJ, 2010) p. 197.

²V. L. Granatstein and G. S. Nusinovich, *J. Appl. Phys.* **108**, 063304 (2010).

³G. S. Nusinovich, R. Pu, T. M. Antonsen, Jr., O. V. Sinit-syn, J. Rodgers, A. Mohamed, J. Silverman, M. Al-Sheikhly, Y. S. Dimant, G. M. Milikh, M. Yu. Glyavin, A. G. Luchinin, E. A. Kopelovich, and V. L. Granatstein, *J. Infrared, Millimeter, Terahertz Waves*, vol. 32, 380-402 (March 2011)

⁴L. G. Cristophorou, D. L. McCorkie, and A. A. Christodoulides, *Electron-Molecule Interactions*, edited by L. G. Cristophorou (Academic, Orlando, 1983), pp. 478-618.

⁵G. S. Nusinovich, G. M. Milikh, and B. Levush, *J. Appl. Phys.* **80**, 4189 (1996).

⁶A. V. Gurevich, N. D. Borisov, and G. M. Milikh, *Artificially Ionized Regions in the Atmosphere* (Gordon and Breach, Reading, UK, 1997).

⁷S. Gold and G. S. Nusinovich, *Rev. Sci. Instrum.* **68**, 3945 (1997).

⁸D. Clunie, G. Mesyats, M. Osipov, M. Petelin, P. Zagulov, S. Korovin, C. Clutterbuck, and B. Wardrop, *Strong Microwaves in Plasmas*, edited by A. G. Litvak (Inst. Appl. Physics, Nizhny Novgorod, 1996), Vol. 2, p. 886.

⁹M. T. Ngo, B. G. Danly, R. Myers, D. E. Pershing, V. Gregers-Hansen, and G. Linde, 3rd Int. Vacuum Electronics Conf., (IEEE, Piscataway, NJ, 2002) p. 363.

¹⁰K. Sakamoto, A. Kasugai, K. Takahashi, R. Minami, N. Kobayashi, and K. Kajiura, *Nat. Phys.* **3**, 411 (2007).

¹¹V. A. Flyagin, A. G. Luchinin, and G. S. Nusinovich, *Int. J. Infrared Millim Waves* **4**, 629 (1983).